Review

^{195}Pt NMR spectroscopy: A chemometric approach*

Elisabetta Gabano, Emilio Marengo, Marco Bobba, Elisa Robotti,
Claudio Cassino, Mauro Botta, Domenico Osella *

Dipartimento di Scienze dell'Ambiente e della Vita, Università del Piemonte Orientale "A. Avogadro", Via Bellini 25/G, 15100 Alessandria, Italy

Contents

Abstract

The growing number of studies on platinum(II) complexes is stimulated by their importance as antitumour chemotherapeutics. ^{195}Pt NMR spectroscopy is a very useful tool for characterizing and investigating these complexes. An accurate estimation of NMR chemical shifts plays an important role in the evaluation of molecular structure. Moreover, the predictions should be fast and accurate in order to be useful as a tool for structure evaluation within a large set of compounds. In this context, ab initio calculations are time consuming and quite difficult because of the relativistic effect that must be considered for the third row transition metals. A new approach is offered here by chemometrics: by means of an artificial neural network algorithm, it is now possible to build a model to predict the chemical shift of a Pt-complex on the basis of its molecular features, thus providing a useful alternative to computational methods. We have successfully applied such a model to 185 different ^{195}Pt chemical shift values.
© 2006 Elsevier B.V. All rights reserved.

Keywords: ^{195}Pt chemical shift; NMR; Platinum complexes; Antitumour drugs; Artificial neural network

1. Introduction

In 1965 Barnett Rosenberg and coworkers at Michigan State University discovered the antitumour properties of cisplatin while investigating the influence of an electric field on cell division. Following its serendipitous discovery, cisplatin was approved by the Food and Drug Administration for the treatment of genitourinary tumours in 1978. Cisplatin provided good results in the treatment of solid tumours and its effectiveness against several types of cancer has made it one of the most widely used anticancer drugs. Its significant side effects, however, induced and still spur researchers to look for new Pt(II) complexes which retain the same activity of cisplatin but exhibit minor drawbacks, by replacement of the leaving groups (chlorides) as well as of the carrier groups (ammonia molecules). These efforts produced two new worldwide approved and two
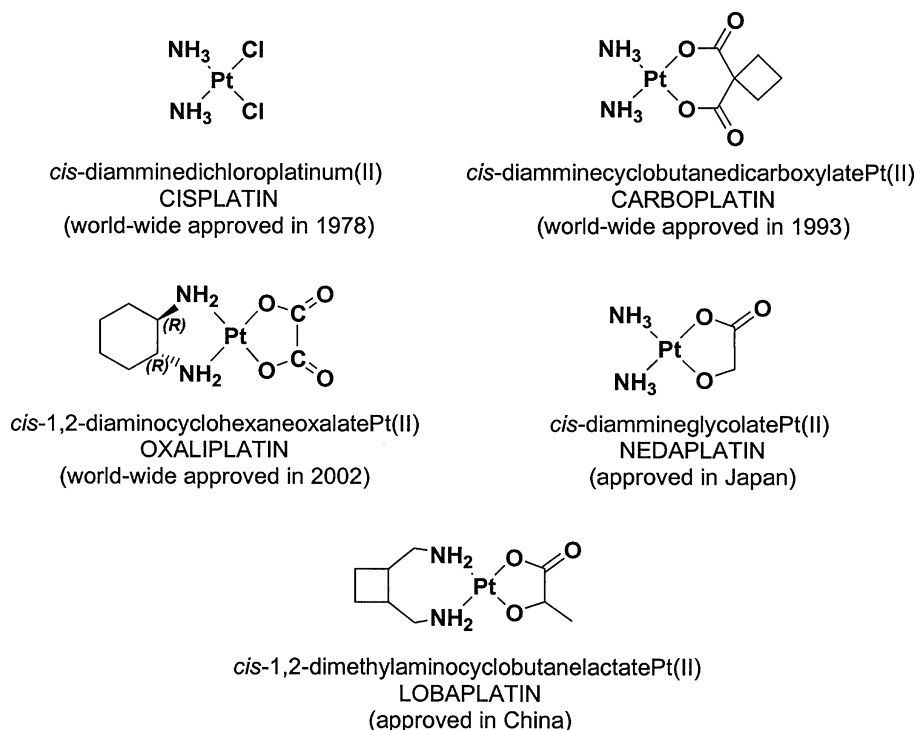
Fig. 1. Platinum anticancer drugs.

regionally approved cisplatin-like derivatives, namely carboplatin, oxaliplatin, nedaplatin and loboplatin (Fig. 1).

Due to the importance of these derivatives as antitumour agents, many new complexes have been synthesized in recent years to try and obtain a better understanding of the relationship between structure and pharmacological activity. An important step of these studies is the characterization of the complexes and NMR, not surprisingly, plays an important role. In particular [195]Pt NMR spectra have been largely utilized owing to a number of favourable spectral properties [1].

[195]Pt chemical shifts cover a wide range of values, about 15,000 ppm, from +8000 to −7000 ppm relative to $\delta[PtCl_6]^{2-} = 0$. Typically, it is possible to discriminate Pt(II) complexes which resonate at low frequencies from Pt(IV) complexes which resonate at high frequencies. Many factors influence the shielding of a heavy atom like [195]Pt: the nature of the ligands present in the coordination sphere, their spatial arrangement, the nature of the bound donor atoms, concentration, pH, temperature and solvent effects [2,3]. The identity and the purity of the platinum complexes are usually verified by [195]Pt NMR spectroscopy, since each species shows one characteristic signal only.

There are some practical difficulties to be faced when recording a [195]Pt NMR spectrum. Considering the magnetic field strength typical of modern equipments (7.05–11.75 T) two principal problems are the exceedingly large spectral range to be excited and the acoustic ringing [4,5].

These practical aspects suggest the need of predictive tools able to define a limited chemical shift range on which the spectroscopist can focus.

The easiest approach to the [195]Pt chemical shift prediction is to draw some practical deductions from series of experimental data [6,7]. Appleton et al. [6], for example, studied a series of $Pt(^{15}NH_3)_3Z^{n+}$ complexes and drew some qualitative conclusions based on the assumption of the additive effect of the ligand substitution. Kennedy et al. [8] studied organoplatinum compounds and pointed out some empirical trends, which were in part explained in terms of the chemico-physical properties of the complexes under study. Beyond the qualitative trends we can draw from experimental data, we are interested in a more quantitative approach to $\delta(Pt)$ prediction. Few computational studies on [195]Pt chemical shifts exist: the theoretical prediction of the [195]Pt chemical shift is not an easy task, because it requires consideration of the relativistic effects. Öhrström [9] reported on the correlation between transition metal NMR chemical shifts and the stability of coordination compounds.

In the past 40 years some theoretical $\delta(Pt)$ rationalization and prediction studies have been made. Pidcock et al. [10], Goggin et al. [11] and Dean and Geen [12] applied Ramsey's equation [13] for paramagnetic shielding to different platinum complexes. Koie et al. [14] studied some acetyleneplatinum(0) complexes and explained the results semiquantitatively through charge-iterative extended Hückel molecular-orbital calculations. Gilbert and Ziegler [15] used the density functional theory (DFT) with relativistic corrections to calculate the [195]Pt chemical shift for a series of neutral *cis*- and *trans*-PtX_2L_2 complexes. Both the paramagnetic and the spin–orbit-shielding contributions were important for determining the [195]Pt chemical shift.

Owing to the difficulties intrinsic in the computational approaches, a simpler $\delta(Pt)$ prediction method may be a useful tool for the synthetic chemist for evaluating the success

or the failure of a particular platinum complex synthesis, for discriminating between coordination isomers [16,17] and for determining the enantiomeric purity and absolute configuration of Pt-coordinated enantiomers [18].

We have focused our attention on a different approach for predicting the [195]Pt chemical shift. Chemometrics offers a new answer to the problem of chemical shift prediction. The chemometric method tries to correlate the [195]Pt chemical shifts from literature data to particular molecular features. Since we are interested in cisplatin-like complexes, in our study we considered cis-[A$_2$PtX$_2$] complexes (A = amine, A$_2$ = diamine, X = I, Cl, carboxylate, X$_2$ = dicarboxylate) because they are the products (especially chloride- and dicarboxylate-derivatives) or the intermediates (especially iodide-derivatives in the Dhara's approach [19]) in the syntheses of antitumour agents. First of all, we identified some simple molecular features that could be related to the chemical shift, such as the type of coordinated atoms, the nature of coordinated amines or carboxylates, and the solvent used for the measurement. We employed an 'artificial neural network' (ANN) approach to predict the [195]Pt chemical shift. In the past years ANNs were successfully used to predict ^{1}H and ^{13}C NMR chemical shifts [20–26], but they represent a new method of calculation in the field of [195]Pt chemical shift.

2. Prediction of [195]Pt chemical shifts: the chemometric approach

The [195]Pt chemical shifts of a number of cis-[A$_2$PtX$_2$] complexes (A = amine, A$_2$ = diamine, X = I, Cl, carboxylate, X$_2$ = dicarboxylate), reported in the literature as products or intermediates in the syntheses of antitumour agents, have been treated here with several chemometric methods in order to predict δ(Pt) by correlating it with some molecular features [the type of coordinated atoms, the nature of coordinated amines (chelating or not, aliphatic, aromatic, primary, secondary...) and carboxylates (chelating or not, substituted on the α-carbon or not...), and the solvent used for the measurement]. An ANN algorithm was finally used to predict the [195]Pt chemical shift.

2.1. [195]Pt chemical shift data and variables

The chemical shifts of the Pt(II) complexes considered here were obtained from the literature (Table 1) [27–57]. All the δ(Pt) values were referenced to δ(K$_2$PtCl$_4$) = −1628 ppm.

We identified some simple molecular features that are likely related to the chemical shift and encoded them in the form of the variables listed in Table 2.

The original set of 31 descriptors was reduced to 28 variables eliminating N3, O2 and O3 because they are constant over the whole set of Pt(II) complexes under investigation.

2.2. Artificial neural networks

Artificial neural networks [58,59] are mathematical algorithms that can be used to solve complex problems by simulating the function of the human brain. They are mainly dedicated to modelling the behaviour of complex systems where they usu-

ally provide better results than ordinary least squares (OLS), especially when non-linear relationships are present. The main problem when applying ANN is overfitting and this must be handled with particular care.

In the present work two types of neural networks were applied: supervised and unsupervised networks.

Supervised back-propagation artificial neural networks (BP-ANN) build models, which classify patterns and make predictions according to other patterns of input and output they have learned [60–64]. Unsupervised artificial neural networks can group the objects of a dataset into different classes, on the basis of their similarity. A Kohonen network, also called a self-organising map (SOM), employed here for experimental design purposes, is a typical unsupervised network [65–70].

2.3. Back-propagation networks

The back-propagation network is the most popular ANN used for calibration; it consists of:

- an input layer, where each neuron is associated with an experimental variable (in this case the molecular features);
- one or more hidden layers with a variable number of neurons;
- an output layer, where each neuron is associated with a response (in this case the [195]Pt chemical shift).

In the back-propagation training algorithm the signal moves from the input layer towards the output layer. In this process each neuron uploads all the neurons of the successive layer, transferring a portion of the value (input) it has accumulated. The portion of signal that is transferred is regulated by a transfer function (Fig. 2).

The choice of the network architecture (Fig. 3) is very important because it determines the ability of the network to predict unknown responses; it consists in selecting the number of hidden layers, the number of neurons in each hidden layer, the neuron's connection pattern and the specific transfer functions to be applied between the different neuron layers.

In this work only one hidden layer containing five neurons and the logistic transfer function were selected (Fig. 2A).

The back-propagation algorithm attempts to minimize the difference (or error) between the desired and actual output in an iterative manner. For each iteration, the initial weights involved in the network are adjusted by the algorithm so that the error is decreased along a descending direction. Two parameters, called learning rate (set here to 0.3) and momentum (set here to 0.1), are used for controlling the size of weight adjustment along the descending direction and for dampening oscillations of the iterations.

The secret of building successful neural networks is to know when to stop the training. In fact if the net is trained too quickly it will not learn the data patterns while if the net is trained for too long, it will learn the noise and memorize the data (overfitting). The real power of neural networks is evident when the trained network is able to produce good results for new data which means that the general rules governing the investigated system have been understood and incorporated by the ANN; this is the

Table 1
Pt(II) complexes and the corresponding δ(Pt) values

No.	Compound	δ(Pt), ppm	Ref.	No.	Compound	δ(Pt), ppm	Ref.
1		−2345 (−2340)	[27]	2		−2433 (−2391)	[28]
3		−2355 (−2327)	[28]	4		−2386 (−2313)	[28]
5		−2168 (−2097)	[28]	6		−2219 (−2175)	[28]
7		−2290 (−2247)	[28]	8		−2097 (−2097)	[29]
9		−1717 (−1714)	[30]	10		−1708 (−1714)	[30]
11		−1692 (−1714)	[30]	12		−1684 (−1714)	[30]
13		−1708 (−1714)	[30]	14		−2300 (−2391)	[31]
15		−1998 (−1991)	[32]	16		−3199 (−3217)	[32]
17		−2014 (−1991)	[32]	18[a]		−3274 (−3217)	[32]
19		−3228 (−3217)	[32]	20		−2011 (−1991)	[32]
21		−2008 (−1991)	[32]	22		−3199 (−3217)	[32]

Table 1 (*Continued*)

No.	Compound	δ(Pt), ppm	Ref.	No.	Compound	δ(Pt), ppm	Ref.
23[a]		−3296 (−3217)	[32]	24		−2021 (−1991)	[32]
25		−3205 (−3217)	[32]	26		−2003 (−1991)	[32]
27		−2188 (−2247)	[33]	28		−3211 (−3348)	[33]
29		−2224 (−2247)	[33]	30		−2222 (−2247)	[33]
31		−2184 (−2247)	[33]	32		−2242 (−2247)	[33]
33		−2208 (−2247)	[33]	34		−2213 (−2247)	[33]
35		−2199 (−2247)	[33]	36		−2188 (−2247)	[33]
37		−2230 (−2247)	[33]	38		−2219 (−2247)	[33]
39		−2223 (−2247)	[33]	40		−2235 (−2247)	[33]
41		−2104 (−2097)	[32]	42		−2235 (−2247)	[33]
43		−1965 (−1991)	[32]	44		−3330 (−3348)	[33]
45		−3327 (−3348)	[33]	46		−3462 (−3368)	[33]
47		−3364 (−3348)	[33]	48		−3333 (−3348)	[33]

Table 1 (*Continued*)
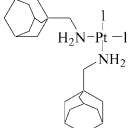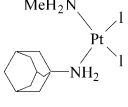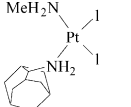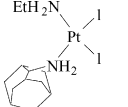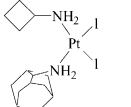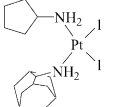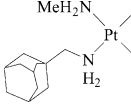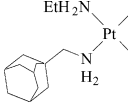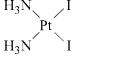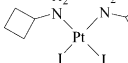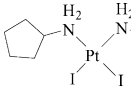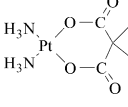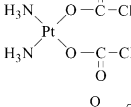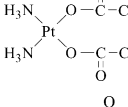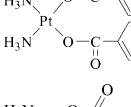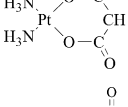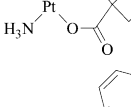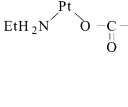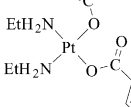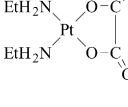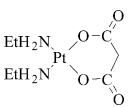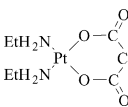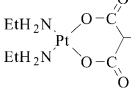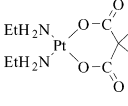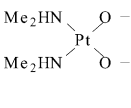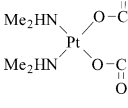
No.	Compound	δ(Pt), ppm	Ref.	No.	Compound	δ(Pt), ppm	Ref.
49		−3354 (−3348)	[33]	50		−3336 (−3348)	[33]
51		−3328 (−3348)	[33]	52		−3327 (−3348)	[33]
53		−3387 (−3348)	[33]	54		−3328 (−3348)	[33]
55		−3389 (−3348)	[33]	56		−3388 (−3348)	[33]
57		−3264 (−3316)	[33]	58		−3346 (−3348)	[33]
59		−3302 (−3348)	[33]	60		−1714 (−1758)	[34]
61		−1615 (−1602)	[35]	62		−1565 (−1602)	[35]
63		−1552 (−1595)	[35]	64		−1686 (−1733)	[35]
65		−1720 (−1758)	[35]	66		−1705 (−1702)	[35]
67		−1730 (−1694)	[35]	68		−1872 (−1923)	[35]
69		−1873 (−1931)	[35]	70		−1827 (−1863)	[35]
71		−1833 (−1863)	[35]	72		−1860 (−1892)	[35]
73		−1693 (−1702)	[35]	74		−1615 (−1694)	[35]

Table 1 (*Continued*)

No.	Compound	δ(Pt), ppm	Ref.	No.	Compound	δ(Pt), ppm	Ref.
75	(structure)	−1887 (−1923)	[35]	76	(structure)	−1882 (−1931)	[35]
77	(structure)	−1826 (−1863)	[35]	78	(structure)	−1835 (−1863)	[35]
79	(structure)	−1869 (−1892)	[35]	80	(structure)	−1683 (−1677)	[35]
81	(structure)	−1675 (−1677)	[35]	82	(structure)	−1838 (−1774)	[35]
83	(structure)	−1816 (−1765)	[35]	84	(structure)	−1988 (−2011)	[35]
85	(structure)	−1974 (−2021)	[35]	86	(structure)	−1923 (−1949)	[35]
87	(structure)	−1926 (−1949)	[35]	88	(structure)	−1964 (−1979)	[35]
89	(structure)	−1777 (−1765)	[35]	90	(structure)	−1706 (−1756)	[35]
91	(structure)	−1970 (−1999)	[35]	92	(structure)	−1976 (−2009)	[35]
93	(structure)	−1922 (−1938)	[35]	94	(structure)	−1930 (−1938)	[35]
95	(structure)	−1966 (−1967)	[35]	96	(structure)	−1581 (−1602)	[36]
97	(structure)	−1694 (−1733)	[35]	98	(structure)	−1723 (−1758)	[35]
99	(structure)	−3636 (−3500)	[27]	100	(structure)	−2282 (−2247)	[37]
101	(structure)	−1978 (−1923)	[37]	102	(structure)	−1966 (−1931)	[37]

Table 1 (*Continued*)

No.	Compound	δ(Pt), ppm	Ref.	No.	Compound	δ(Pt), ppm	Ref.
103		−1971 (−1863)	[37]	104		−1900 (−1892)	[37]
105		−1955 (−1863)	[37]	106		−1895 (−1892)	[37]
107		−1953 (−1892)	[37]	108		−2346 (−2367)	[38]
109		−2354 (−2367)	[38]	110		−2163 (−2175)	[38]
111		−2163 (−2175)	[38]	112		−2163 (−2175)	[38]
113		−2338 (−2367)	[39]	114		−2342 (−2367)	[39]
115		−2343 (−2367)	[39]	116		−2341 (−2367)	[39]
117		−3115 (−3217)	[40]	118		−2000 (−2045)	[41]
119		−2078 (−2045)	[41]	120		−2010 (−2059)	[42]
121		−2041 (−2031)	[42]	122		−1990 (−2014)	[42]
123		−2005 (−1985)	[42]	124		−2006 (−1967)	[42]
125		−2031 (−1938)	[42]	126		−3304 (−3335)	[43]

Table 1 (*Continued*)

No.	Compound	δ(Pt), ppm	Ref.	No.	Compound	δ(Pt), ppm	Ref.
127		−2162 (−2175)	[43]	128		−1844 (−1933)	[44]
129		−1873 (−1933)	[44]	130		−1884 (−1859)	[44]
131		−1917 (−1859)	[44]	132[b]		−2114 (−2103)	[45]
133[c]		−2125 (−2103)	[45]	134		−1932 (−1914)	[46]
135		−1922 (−1914)	[46]	136		−1939 (−1914)	[46]
137		−1815 (−1838)	[47]	138		−1928 (−1859)	[47]
139		−2035 (−2045)	[48]	140		−1918 (−1991)	[48]
141		−2208 (−2146)	[49]	142		−1831 (−1833)	[49]
143		−1859 (−1841)	[49]	144		−1622 (−1779)	[49]
145		−1863 (−1779)	[49]	146		−1859 (−1806)	[49]
147		−2357 (−2367)	[50]	148		−2361 (−2367)	[50]
149		−2359 (−2367)	[50]	150		−3313 (−3369)	[50]
151		−3313 (−3369)	[50]	152		−1996 (−2026)	[50]
153		−1989 (−2023)	[51]	154		−2284 (−2340)	[51]

Table 1 (*Continued*)

No.	Compound	δ(Pt), ppm	Ref.	No.	Compound	δ(Pt), ppm	Ref.
155[b]		−2287 (−2340)	[52]	156[b]		−1995 (−2023)	[52]
157		−1732 (−1733)	[53]	158		−1719 (−1733)	[53]
159		−1741 (−1733)	[53]	160		−1748 (−1733)	[53]
161		−1754 (−1733)	[53]	162		−1719 (−1733)	[53]
163		−1714 (−1733)	[53]	164		−1976 (−1960)	[53]
165		−1964 (−1960)	[53]	166		−1903 (−1960)	[53]
167		−1900 (−1960)	[53]	168		−1790 (−1795)	[53]
169		−1784 (−1795)	[53]	170		−2094 (−2097)	[53]
171		−1716 (−1758)	[53]	172		−2360 (−2367)	[54]

Table 1 (*Continued*)

No.	Compound	δ(Pt), ppm	Ref.	No.	Compound	δ(Pt), ppm	Ref.
173		−2019 (−1971)	[55]	174		−1983 (−1981)	[55]
175		−1992 (−1910)	[55]	176		−1918 (−1940)	[55]
177		−2088 (−1940)	[55]	178		−1935 (−1910)	[55]
179		−1895 (−1940)	[55]	180		−1947 (−2042)	[55]
181		−2267 (−2247)	[56]	182		−1838 (−1884)	[56]
183		−2347 (−2367)	[57]	184		−2354 (−2367)	[57]
185		−3247 (−3316)	d				

No. identifies the Pt(II) complex and the experimental conditions (solvent) employed for obtaining δ(Pt). The observed δ(Pt) values are on the left, those predicted using the ANN model (17 variables) are on the right in brackets.

^a Means of two rotamers.
^b (R,R) + (S,S).
^c (R,S) + (S,R).
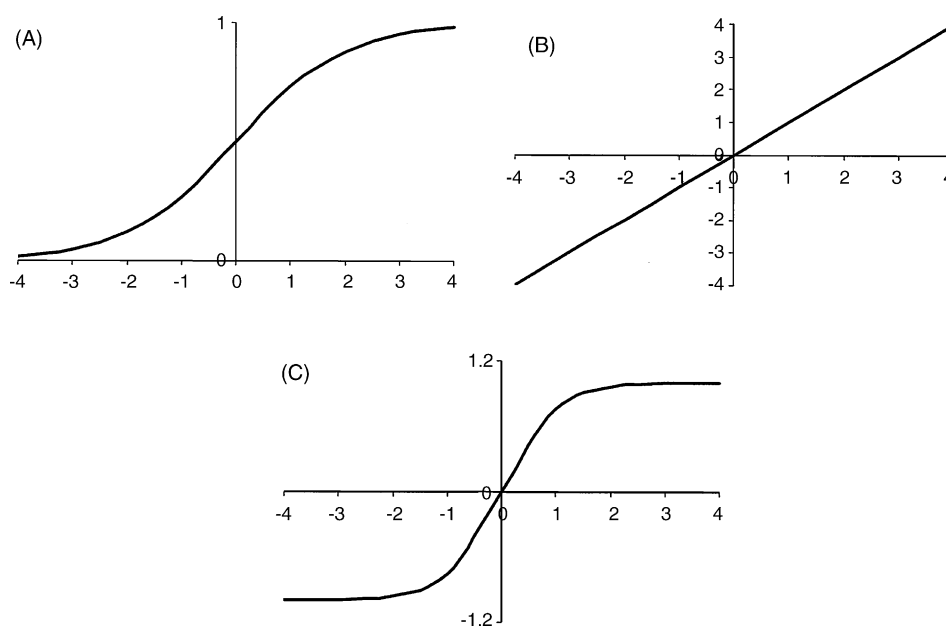^d Measured in DMF-d$_7$ purposely for this work.

Fig. 2. Transfer function: (A) logistic; (B) linear; (C) hyperbolic tangent.

Table 2
Variables

Variable	Description
S1	S1 = 1 if the solvent is D_2O or CD_3OD, S1 = 0 otherwise
S2	S2 = 1 if the solvent is DMF-d_7, S2 = 0 otherwise
S3	S3 = 1 if the solvent is DMSO-d_6, S3 = 0 otherwise
S4	S4 = 1 if the solvent is $CDCl_3$ or CD_2Cl_2, S4 = 0 otherwise
N0	Number of coordinated NH_3
N1	Number of primary nitrogen atoms in non-chelating amines
N2	Number of secondary nitrogen atoms in non-chelating amines
N3	Number of tertiary nitrogen atoms in non-chelating amines
NA	Number of aromatic nitrogen atoms in non-chelating amines
NC1	Number of primary nitrogen atoms in chelating amines
NC2	Number of secondary nitrogen atoms in chelating amines
NC3	Number of tertiary nitrogen atoms in chelating amines
nN5	Number of five-membered X_2–N–Pt–N rings (X = any atom)
nN6	Number of six-membered X_3–N–Pt–N rings
nN7	Number of seven-membered X_4–N–Pt–N rings
Cl	Number of chloride atoms
I	Number of iodide atoms
O1	Number of oxygen atoms in non-chelating carboxylates with primary carbon in α position relative to C=O
O2	Number of oxygen atoms in non-chelating carboxylates with secondary carbon in α position relative to C=O
O3	Number of oxygen atoms in non-chelating carboxylates with tertiary carbon in α position relative to C=O
O4	Number of oxygen atoms in non-chelating carboxylates with quaternary carbon in α position relative to C=O
OA	Number of oxygen atoms in non-chelating carboxylates with aromatic carbon in α position relative to C=O
OC2	Number of oxygen atoms in chelating carboxylates with secondary carbon in α position relative to C=O
OC3	Number of oxygen atoms in chelating carboxylates with tertiary carbon in α position relative to C=O
OC4	Number of oxygen atoms in chelating carboxylates with quaternary carbon in α position relative to C=O
OCA	Number of oxygen atoms in chelating carboxylates with aromatic carbon in α position relative to C=O
OCΠ	Number of oxygen atoms in chelating carboxylates with a π system in α position relative to C=O
nO5	Number of five-membered X_2–O–Pt–O rings (X = any atom)
nO6	Number of six-membered X_3–O–Pt–O rings
nO7	Number of seven-membered X_4–O–Pt–O rings
nO8	Number of eight-membered X_5–O–Pt–O rings

basis for obtaining a good prediction ability. In order to resolve the problem of overfitting, the dataset set was split in three sets:

- training set, used for training the network (model building);
- test set, used for selecting the end of the training phase;
- production set, used for testing the predictive ability of the network.

The training set is then used for training the net and obtaining the weights. The net calculated from the training set is applied to the test set to obtain an estimate of the error in prediction. This error is used to decide when to stop the training itself. The final network prediction ability is validated by means of the production set. The samples of the production set do not influence either the back-propagation optimisation of the weights or the selection of the optimal interruption of the training phase; this allows the correct evaluation of the ANN predictive ability.
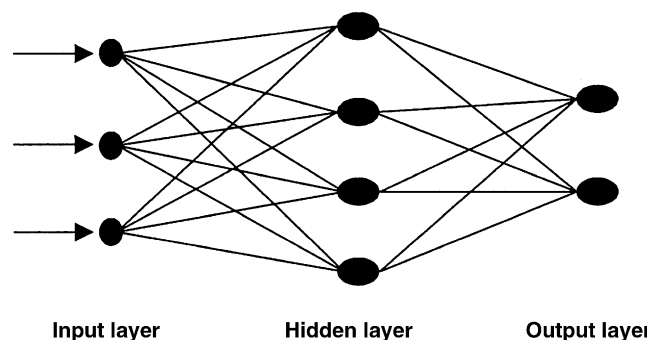

Fig. 3. Schematic representation of artificial neural network architecture.

2.4. Kohonen self-organising maps

The Kohonen ANN is based on a single layer of neurons arranged in a box exhibiting a two-dimensional plane of responses on its top and a vector of weights below each neuron of the top-map. There is typically one weight for every input variable. During the learning each input vector is compared with the weights of every neuron and, as a rule, only the neuron closest to the input vector is activated, giving rise to so-called *competitive learning*. After the winning neuron is determined, the weights are corrected. The size of the correction and the distance the correction extends from the winning neuron define the learning process. The learning procedure considers the local feedback only, which may change if, during learning, the distance affected by the correction does change. This means that only a small number of neurons are involved in the correction of the weights: the ones that are topologically closer to the winning neuron. Such local feedback causes the topologically closer neurons to start acting similarly, if similar input objects are presented to the network. This means that two similar objects will excite two topologically close neurons and two very different objects will excite the winning neurons topologically far away from each other.

The final result is a map, the first layer, where the most similar samples are in the same cell or in topologically close cells. The weights give insight into the reason for the aggregation of the objects. So the analysis of the first layer provides information on the similarity of the samples while the analysis of the weights provides information on the reason for their similarity.

A total of 500 iterations were used, with the learning rate decreasing linearly from 0.5 to 0.01. At the same time the range of the correction weights is decreased from the maximum range to zero, which implies that in the last learning cycles only the winning neuron weights were updated.

The starting weights were initialized with small random numbers in the range 0–0.2 and the data were range scaled in the interval 0.2–0.8.

2.5. Index for estimating fitting and prediction ability

The fitting ability of artificial neural models was evaluated by the coefficient of multiple determination, R^2, calculated as:

$$R^2 = 1 - \sqrt{\frac{\sum_{i=1,n}(\widehat{y}_i - y_i)^2}{\sum_{i=1,n}(y_i - \bar{y})^2}}$$

where the two sums run on the number of samples n of the training set, $\hat{y}_i$ is the predicted value of the response for the ith experiment, y_i the experimental value for the ith experiment and $\bar{y}$ is the average response of n experiments. An analogous expression was used to evaluate the predictive ability of the models, using the production set experiments, in which case the two sums of squares run on the experiments of the production set.

The root mean square error (RMSE) between the measured and predicted values is estimated as:

$$\text{RMSE} = \sqrt{\frac{\sum_i (\hat{y}_i - y_i)^2}{n}}$$

that again can be calculated using both training (RMSEF, root mean square error of fitting) or production (RMSEP, root mean square error of prediction) set experiments, to achieve information about fitting and predicting ability.

3. Results and discussion

The Kohonen network was used to select the training set [71–74]. The aim was to find the samples that guaranteed a homogenous representation of the whole experimental domain. For this purpose the 185 samples were the input for a $15 \times 15 \times 28$ Kohonen network; the net was trained for 500 epochs, which resulted in convergence so that the configuration of the first layer (top-map) did not change anymore. In the end the samples were assigned to the cells of the top-map (Fig. 4), on the basis of the similarity of the 28 descriptors. Each cell of the top-map is occupied by the samples more similar, for their variable profile, to the weights of the same cell. Mainly samples assigned to the same cell or to adjacent cells are more similar between them than with respect to samples belonging to cells that are far away on the top-map.

Not all the neurons (cells) were occupied. When a cell was occupied by only one sample, this sample was selected for the

Table 3
Number of objects in the training, test and production sets

Set	Number of objects
Training set	93
Test set	55
Production set	37

training set. When more than one sample with a different values of ^{195}Pt chemical shift was present in a cell, approximately 1/3 of the samples were selected for the training set. The samples not selected for the training set were randomly put in the test and production set.

The number of objects inserted in the three sets is listed in Table 3.

Among the neural networks investigated (1–3 hidden layers with 1–10 neurons each), the one that provided the best results contained only one hidden layer with five neurons.

First an ANN with the whole set of input variables was trained. The final back-propagation artificial neural network had a coefficient of multiple determination of 0.99 for the training set and 0.99 for the production set. The RMSEP was equal to 50.75 and the model performed satisfactorily both in fitting and prediction. The experimental versus predicted chemical shift of the 185 objects is shown in Fig. 5.

Artificial neural networks are often considered as "black boxes". This view stems from the fact that the contribution of the input variables in predicting the value of the output is difficult to disentangle within the network. Consequently, input variables are often entered into the network and an output value is generated without gaining any understanding of the inter-relationships between the variables, and therefore without gaining any explanatory insight into the underlying mechanisms being modelled by the network.
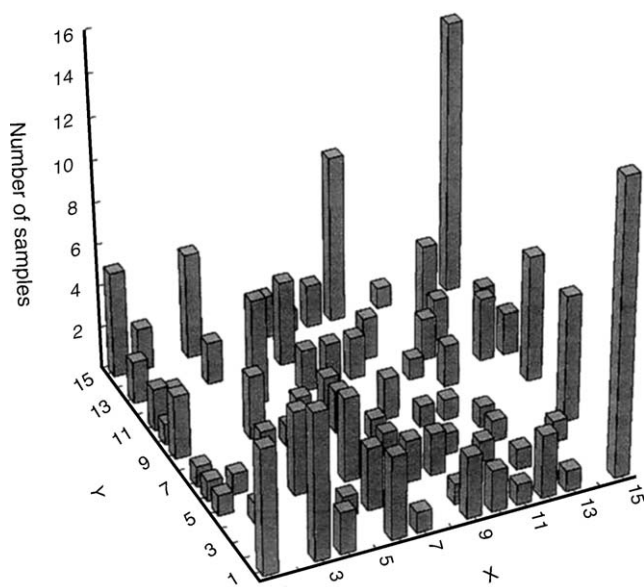

Fig. 4. Occupation of the 15×15 Kohonen top-map.
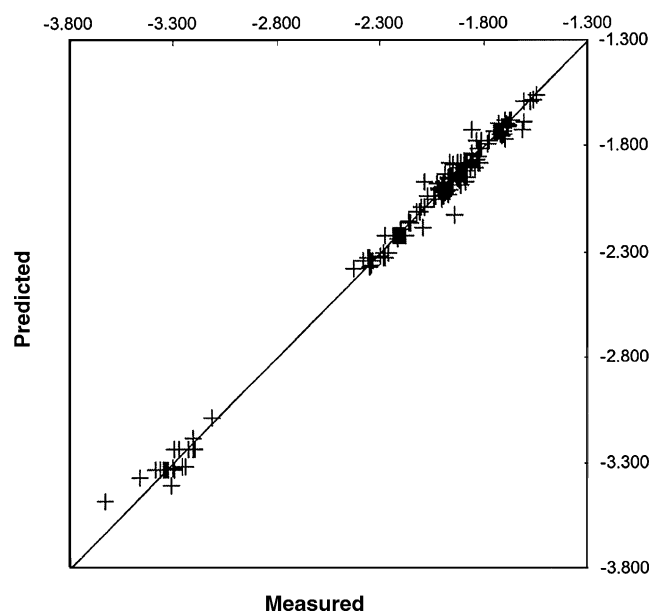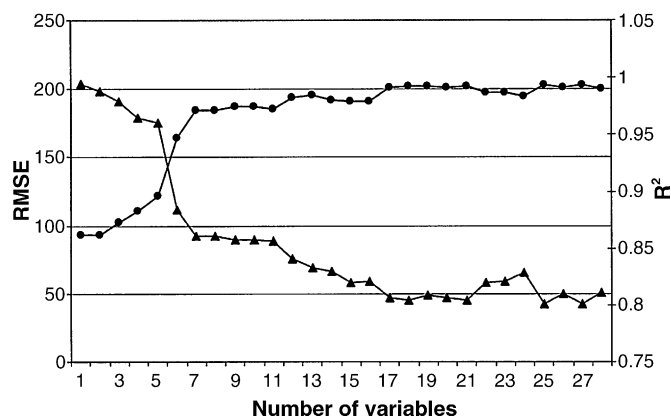

Fig. 5. Predicted vs. experimental ^{195}Pt chemical shifts.

Fig. 6. Trend of R^2 and RMSE for the production set in function of the number of variables.

Fig. 7. Predicted vs. experimental ^{195}Pt chemical shifts of the simplified model.

In order to achieve information about the role played by the input variables in modelling the response, the first derivative of the final network with respect to each input variable for the 185 experimental points available was calculated. In this way it was possible to evaluate the influence that every input variable has on chemical shift, through the neural mathematical model.

The graphs in the Supporting information section report the value of the ANN first derivative with respect to each input variable, versus the scaled value (from 0 to 1) of the corresponding input variable. From these graphs it is possible to observe which variables have more influence on the ^{195}Pt chemical shift. The network derivative applied to ^{195}Pt chemical shifts shows that many input variables do not play a relevant role; in fact they exhibit a first derivative which is constant, around zero. These variables are: S1, S3, S4, N1, NC1, OCA, nO6 and nO7. Instead, positive constant values of the first derivative mean that the variable has a positive linear influence on the response, therefore, if the input variable increases also ^{195}Pt chemical shift increases. The same reasoning can be applied to a negative constant value of the derivative. The variables that show a positive linear effect are: N0, NA, nN7, O1, O4, OA, OC2, OC3, OC4, OCΠ, nO5 and nO8 while the variables that have a negative linear effect are S2, N2, NC2, NC3, nN5, nN6 and Cl.

In some cases calculation of the first derivative shows more complex trends due to more complex relationships between input and output variables (for example quadratic and cubic relations). This is the case of I, for example (see Supporting information).

The BP-ANN model was simplified by taking into consideration these results.

Fig. 6 shows the trend of the coefficient of multiple determination and of the RMSE for the production set obtained with BP-ANN derived by adding, one by one, the input variables in order of relevance, according to the network derivative (see Supporting information). This means that the first variables to be added have the larger absolute value (larger influence on the response) on the first derivative.
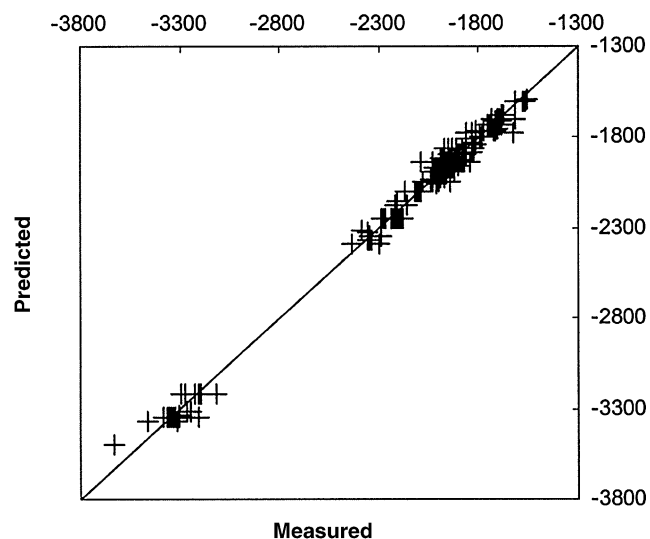
Fig. 6 reports the RMSE and R^2 values obtained for ANN based on an increasing number of descriptors. The most parsimonious but still effective model is searched for.

From Fig. 6 it is possible to observe that the optimal number of variables corresponds to 17, namely the simplest model with optimal RMSE and R^2 values. Table 4 shows the 17 selected variables which are a reduction of the variables in Table 2.

The final BP-ANN trained with only 17 variables out of the 28 available, has a coefficient of multiple determination for both training set and production set of 0.99. In this case the RMSEP is equal to 46.87, which is better that the one obtained with all variables, showing that the inclusion of non-relevant information in the first BP-ANN model, caused a loss of predictive ability and consequent overfitting.

The experimental versus predicted chemical shift and residuals of the whole dataset are shown in Figs. 7 and 8, respectively. The similarity of Figs. 5 and 7 confirms that the elimination of the non-relevant descriptors did not affect the ANN model prediction ability. The final RMSEP is very similar to the experimental uncertainty of the experimental response, while the absence of trends or outliers in the plot of the residuals shows that there is no evident lack-of-fit so that the BP-ANN model is very satisfactory. It is possible to apply this final model to new molecules using a suitable Excel file (available on request).

Among the selected variables there are Cl, I and some descriptors related to the nature of the carboxylate ligands (O-variables), indicating that the type of leaving group is essential for determining the ^{195}Pt prediction. From the analysis of the selected O-variables, it is clear that there are differences between chelating and non-chelating ligands. Substitution on the α carbon with respect to a carboxylic group is also important. Fully substituted and unsubstituted ligands are significantly different, whereas a partial substitution has a marginal effect.

Table 4
Variables selected to build the simplified model

I	O4	OA	O1	nO8	Cl	OCΠ	NA	NC2	nN7	OC4	OC3	nN5	nO5	N2	N0	S2
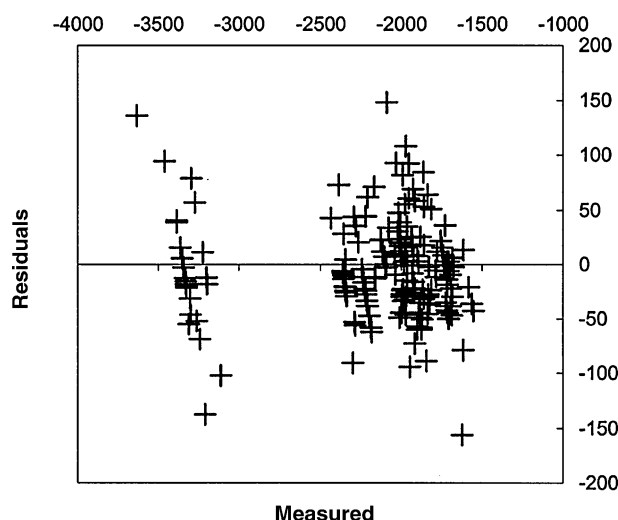
Fig. 8. ^{195}Pt chemical shift residuals of the simplified model.

Fig. 9. *cis*-[Diamino[2-(4-(17α-ethynylestradiolyl)-benzoylamino)-malonato] platinum(II)].

The presence of an aromatic non-chelating ligand is important both for leaving and carrier groups, as well as the presence of a π system in an α position with respect to a carboxylic group.

A solvent effect is evident for DMF. Actually, for some iodide complexes there are noteworthy differences between the ^{195}Pt chemical shift in this solvent and that observed in DMSO.

The variable I has complex relationships with the response. The iodide complexes have lower chemical shifts with respect to the other leaving ligands examined. It is known that the halides are increasingly affected by spin–orbit-coupling, descending the halogen family. This results in an increase in the Pt shielding and in a negative contribution to the chemical shift.

3.1. Application of the chemometric method to coordination isomers

The chemometric model was applied to the prediction of the chemical shift of *cis*-[Diamino[2-(4-(17α-ethynylestradiolyl)-benzoylamino)-malonato]platinum(II)] (**1**) [75], whose plat-
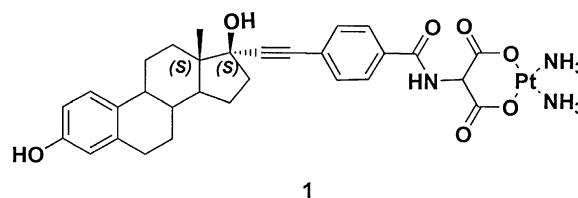
inum centre is coordinated by two amine nitrogen atoms and two carboxylic oxygen atoms (Fig. 9). The ^{195}Pt spectrum of complex **1** run in (CD$_3$)$_2$SO at RT, showed a single signal at −1718 ppm as expected from the chemometric prediction (−1694 ± 47 ppm). On the contrary, the same spectrum in CD$_3$OD at room temperature showed two peaks at −1737 and −2171 ppm, respectively in a 6:1 ratio. The first signal is in agreement with the chemometric prediction for this solvent (−1698 ± 47 ppm), whereas the second is incompatible with the coordination geometry of **1** and must be assigned to a second species originating from **1** in methanol. As previously described by Gibson et al. [17], the presence of a nitrogen atom in α position relative to the malonato unit promotes coordination isomerism of the (O,O′)-chelate **1** to the (N,O)-chelate.

Gibson et al. described the reaction in water between *cis*-[Pt(NH$_3$)$_2$(H$_2$O)$_2$]$^{2+}$ **2** and the barium salt of 2-aminomalonate **3** in water showing that the kinetic product (O,O′)-chelate **4** is formed and is rapidly isomerised to yield the thermodynamically stable (N,O)-chelate **5** (Fig. 10). This isomerisation reaction is pH dependent [76].

We could not measure the spectrum of **1** in D$_2$O because of its poor solubility in this solvent and a direct comparison with the behaviour described by Gibson was not possible. The second signal observed in methanol, however, was very close to that observed by Gibson and coworkers for the (N,O)-chelate. With the hormonal ligand the conversion is slower and more difficult because the amidic nitrogen atom responsible for this isomerisation is less suitable for platinum coordination. The
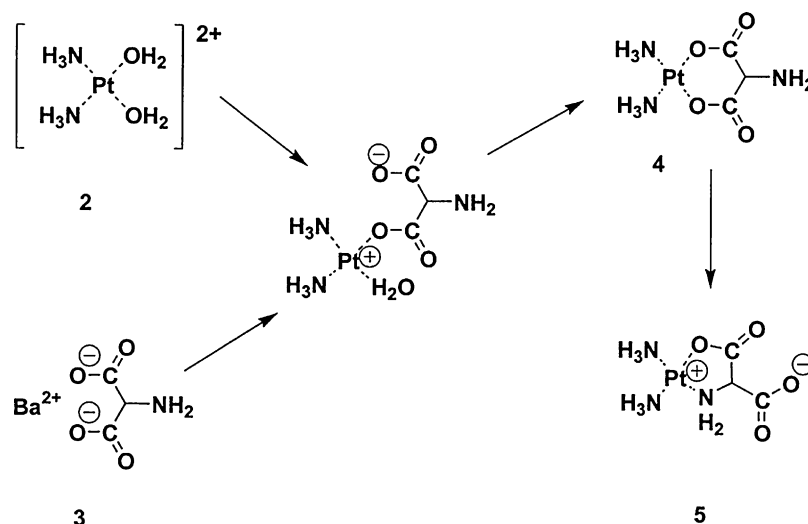

Fig. 10. Isomers of *cis*-[diammino(aminomalonato)platinum(II)].

steric hindrance further inhibits the isomerisation. Thus, the ratio between the (O,O′)-chelate and the (N,O)-chelate is higher for the hormonal derivatives.

This kind of isomerisation is solvent dependent. According to the data reported by Lee et al. [16], the coordination mode of the anionic ligand depends on the hydrogen bonding ability of the solvent with the molecules of the platinum complexes. The (N,O)-chelate is stabilized by protic solvent molecules forming hydrogen bonds with it; whereas the (O,O′)-chelate is more stable in aprotic solvent such as $(CD_3)_2SO$. Methanol has a hydrogen bonding ability that allows the two chelation modes to coexist at room temperature.

This example highlights the importance of ^{195}Pt NMR spectroscopy in association with chemometric methods in the identification and quantification of isomeric distributions in Pt-complexes.

Supplementary material

Network derivatives for the 28 input variables are available. The readers interested in the prediction of ^{195}Pt chemical shift with the ANN model can request an Excel file from these e-mail addresses: marengoe@tin.it (Prof. E. Marengo) or bobba@mfn.unipmn.it (Dr. M. Bobba).

Acknowledgements

Appendix A. Supplementary data

Supplementary data associated with this article can be found, in the online version, at doi:10.1016/j.ccr.2006.02.011.

References

[1] W. Levason, D. Pletcher, Platinum Met. Rev. 37 (1993) 17.
[2] J.J. Pesek, W.R. Mason, J. Magn. Reson. 25 (1977) 519.
[3] W. Freeman, P.S. Pregosin, S.N. Sze, L.M. Venanzi, J. Magn. Reson. 22 (1976) 473.
[4] T.D.W. Claridge, in: J.E. Baldwin, F.R.S. WIlliams, R.M. WIlliams (Eds.), High-Resolution NMR Techniques in Organic Chemistry, Tetrahedron Organic Chemistry Series, vol. 19, Pergamon Press, New York, 1999.
[5] R.K. Harris, Nuclear Magnetic Resonance Spectroscopy: A Physicochemical View, Longman Scientific & Technical, Essex, England, 1986.
[6] T.G. Appleton, J.R. Hall, S.F. Ralph, Inorg. Chem. 24 (1985) 4685.
[7] M. Watabe, M. Kai, S. Asanuma, M. Yoshikane, A. Horiuchi, A. Ogasawara, T. Watanabe, T. Mikami, T. Matsumoto, Inorg. Chem. 40 (2001) 1496.
[8] J.D. Kennedy, W. McFarlane, R.J. Puddephatt, P.J. Thompson, J. Chem. Soc. Dalton Trans. (1976) 874.
[9] L. Öhrström, Comments Inorg. Chem. 18 (1996) 305.
[10] A. Pidcock, R.E. Richards, L.M. Venanzi, J. Chem. Soc. A (1968) 1970.
[11] P.L. Goggin, R.J. Goodfellow, S.R. Haddock, B.F. Taylor, I.R.H. Marshall, J. Chem. Soc. Dalton Trans. (1976) 459.
[12] R.R. Dean, J.C. Geen, J. Chem. Soc. A (1968) 3047.
[13] N.F. Ramsey, Phys. Rev. 78 (1950) 699.
[14] Y. Koie, S. Shinoda, Y. Saito, J. Chem. Soc. Dalton Trans. 5 (1981) 1082.
[15] T.M. Gilbert, T. Ziegler, J. Phys. Chem. A 103 (1999) 7535.
[16] Y.A. Lee, Y.K. Chung, Y.S. Sohn, Inorg. Chem. 38 (1999) 531.
[17] D. Gibson, A. Rosenfeld, H. Apfelbaum, J. Blum, Inorg. Chem. 29 (1990) 5125.
[18] G. Uccello-Barretta, R. Bernardini, F. Balzano, A.M. Caporusso, P. Salvadori, Org. Lett. 3 (2001) 205.
[19] S.C. Dhara, Indian J. Chem. 8 (1970) 193.
[20] D. Svozil, J. Pospíchal, V. Kvasnička, J. Chem. Inform. Comput. Sci. 35 (1995) 924.
[21] D.L. Clouser, P.C. Jurs, Anal. Chim. Acta 321 (1996) 127.
[22] O. Ivanciuc, J.P. Rabine, D. Cabrol-Bass, Comput. Chem. 21 (1997) 437.
[23] J. Meiler, R. Meusinger, M. Will, J. Chem. Inform. Comput. Sci. 40 (2000) 1169.
[24] J. Aires-de-Sousa, M.C. Hemmer, J. Gasteiger, Anal. Chem. 74 (2002) 80.
[25] J. Meiler, W. Maier, M. Will, R. Meusinger, J. Magn. Reson. 157 (2002) 242.
[26] Y. Binev, J. Aires-de-Sousa, J. Chem. Inform. Comput. Sci. 44 (2004) 940.
[27] S.J.S. Kerrison, P.J. Sadler, Inorg. Chim. Acta 104 (1985) 197.
[28] F.D. Rochon, A. Morneau, Magn. Reson. Chem. 29 (1991) 120 (and references therein).
[29] P.S. Pregosin, Coord. Chem. Rev. 44 (1982) 247 (and references therein).
[30] A.R. Khokhar, S. Al-Baker, T. Brown, R. Perez-Soler, J. Med. Chem. 34 (1991) 325.
[31] F.P. Fanizzi, F.P. Intini, L. Maresca, G. Natile, G. Uccello-Barretta, Inorg. Chem. 29 (1990) 29.
[32] C. Tessier, F.D. Rochon, Inorg. Chim. Acta 295 (1999) 25 (and references therein).
[33] F.D. Rochon, M. Doyon, I.S. Butler, Inorg. Chem. 32 (1993) 2717 (and references therein).
[34] O. Aronov, A.T. Horowitz, A. Gabizon, D. Gibson, Bioconj. Chem. 14 (3) (2003) 563.
[35] F.D. Rochon, L.M. Gruia, Inorg. Chim. Acta 306 (2000) 193 (and references therein).
[36] T.G. Appleton, R.D. Berry, C.A. Davis, J.R. Hall, H.A. Kimlin, Inorg. Chem. 23 (1984) 3514.
[37] S.R.A. Khan, I. Guzman-Jimenez, K.H. Whitmire, A.R. Khokhar, Polyhedron 19 (2000) 975.
[38] D. Gibson, N. Mansur, K.F. Gean, J. Inorg. Biochem. 58 (1995) 79.
[39] L.C. Perrin, P.D. Prenzler, C. Cullinane, D.R. Phillips, W.A. Denny, W.D. McFadten, J. Inorg. Biochem. 81 (2000) 111.
[40] R.J. Goodfellow, in: J. Mason (Ed.), Multinuclear NMR, Plenum Press, New York, 1987.
[41] F.D. Rochon, P.C. Kong, R. Melanson, K.A. Skov, N. Farrell, Inorg. Chem. 30 (1991) 4531.
[42] M.S. Ali, K.H. Whitmire, T. Toyomasu, Z.H. Siddik, A.R. Khokhar, J. Inorg. Biochem. 77 (1999) 231.
[43] E.G. Talman, W. Bruning, J. Reedijk, A.L. Spek, N. Veldman, Inorg. Chem. 36 (1997) 854.
[44] I.A. Lee, O.S. Jung, S.J. Kang, K.B. Lee, Y.S. Sohn, Inorg. Chem. 35 (1996) 1641.
[45] R.E. Shepherd, S. Zhang, R. Kortes, F.T. Lin, C. Maricondi, Inorg. Chim. Acta 204 (1996) 15.
[46] Y.A. Lee, Y.K. Chung, Y.S. Sohn, Inorg. Chem. 38 (1999) 531.
[47] Y.A. Lee, O.S. Jung, Y.S. Sohn, Polyhedron 14 (1995) 2099.
[48] M. Van Beusichem, N. Farrell, Inorg. Chem. 31 (1992) 634.

[49] S. Shamsuddin, I. Takahashi, Z.H. Siddik, A.R. Khokhar, J. Inorg. Biochem. 61 (1996) 291.

[50] M.V. De Almeida, E.T. Cesar, E.C.A. Felício, A.P.S. Fontes, M.R. Gero, J. Braz. Chem. Soc. 11 (2000) 154.

[51] J.D. Hoeschele, N. Farrell, W.R. Turner, C.D. Rithner, Inorg. Chem. 27 (1988) 4106.

[52] J.F. Vollano, S. Al-Baker, J.C. Dabrowiak, I.E. Schurig, J. Med. Chem. 30 (1987) 716.

[53] D. Gibson, I. Binyamin, M. Haj, I. Ringel, A. Ramu, J. Katzhendler, Eur. J. Med. Chem. 32 (1997) 823.

[54] S. Ren, L. Cai, B.M. Segal, Dalton Trans. (1999) 1413.

[55] U. Mukhopadhyay, J. Thurston, K.H. Whitmire, Z.H. Siddik, A.R. Khokhar, J. Inorg. Biochem. 94 (2003) 179.

[56] M. Watabe, M. Kai, K. Goto, H. Ohmuro, S. Furukawa, N. Chikaraishi, T. Takayama, Y. Koike, J. Inorg. Biochem. 97 (2003) 240.

[57] Y.S. Kim, K.M. Kim, R. Song, M.J. Jun, Y.S. Sohn, J. Inorg. Biochem. 87 (2001) 157.

[58] J. Zupan, J. Gasteiger, Neural Network for Chemist: an Introduction, John Wiley & Sons, New York, USA, 1993.

[59] M. Hagan, H. Demuth, M. Beale, Neural Network Design, PWS Publishing, Boston, USA, 1996.

[60] B.J. Wythoff, Chemometr. Intell. Lab. Syst. 18 (2) (1993) 115.

[61] B. Walczak, Anal. Chim. Acta 322 (1–2) (1996) 21.

[62] A.T.C. Goh, Artif. Intell. Eng. 9 (3) (1995) 143.

[63] L. Zhang, G. Subbarayan, Comput. Meth. Appl. Mech. Eng. 191 (25–26) (2002) 2873.

[64] L. Zhang, G. Subbarayan, Comput. Meth. Appl. Mech. Eng. 191 (25–26) (2002) 2887.

[65] J. Zupan, M. Novic, I. Ruisanchez, Chemometr. Intell. Lab. Syst. 38 (1) (1997) 1.

[66] W.J. Melssen, J.R.M. Smits, G.H. Rolf, G. Kateman, Chemometr. Intell. Lab. Syst. 18 (2) (1993) 195.

[67] X.H. Song, P.K. Hopke, Anal. Chim. Acta 334 (1–2) (1996) 57.

[68] W.J. Melssen, J.R.M. Smits, L.M.C. Buydens, G. Kateman, Chemometr. Intell. Lab. Syst. 23 (2) (1994) 267.

[69] T. Kohonen, Neurocomputing 21 (1–3) (1998) 1.

[70] T. Kohonen, Self-Organizing Maps, 3rd ed., Springer, Berlin, Germany, 2001.

[71] W. Wu, B. Walczak, D.L. Massart, S. Heuerding, F. Erni, I.R. Last, K.A. Prebble, Chemometr. Intell. Lab. Syst. 33 (1) (1996) 35.

[72] K. Rajer-Kanduc, J. Zupan, N. Majcen, Chemometr. Intell. Lab. Syst. 65 (2) (2003) 221.

[73] E. Marengo, C. Soave, M.C. Gennaro, E. Robotti, M. Bobba, M. Lenti, Ann. Chim. 94 (3) (2004) 219.

[74] E. Marengo, M. Bobba, E. Robotti, M. Lenti, Anal. Chim. Acta 511 (2) (2004) 313.

[75] E. Gabano, C. Cassino, S. Bonetti, C. Prandi, D. Colangelo, A.L. Ghiglia, D. Osella, Org. Biomol. Chem. 3 (2005) 3531.

[76] T.G. Appleton, J.R. Hall, D.W. Neale, C.S.M. Thompson, Inorg. Chem. 29 (1990) 3985.